

## ON THE MODELING AND CHARACTERIZATION OF CRYOGEN SPRAY COOLING FOR APPLICATION TO PORT WINE STAIN LASER THERAPY

Guillermo Aguilar<sup>1,2</sup>, Emil Karapetian<sup>2</sup>, J. Stuart Nelson<sup>1,2</sup>, and Enrique J. Lavernia<sup>3</sup>

<sup>1</sup>Department for Biomedical Engineering, UC, Irvine, CA 92612

<sup>2</sup>Beckman Laser Institute, UC, Irvine, CA 92612

<sup>3</sup>Department of Chemical Engineering and Material Sciences, UC, Irvine, CA 92697

Corresponding author: gaguilar@bli.uci.edu

T: 949-824-3754, F: 949-824-8413

### ABSTRACT

The combination of cryogen spray cooling (CSC) and laser irradiation has proven to be a viable solution to treat various dermatologic vascular disorders, such as port wine stain birthmarks (PWS). PWS patients are treated with laser pulses that induce permanent thermal damage to the target blood vessels. However, absorption of laser energy by melanin causes localized heating of the epidermis, which may result in complications, such as hypertrophy, scarring, or dyspigmentation. By applying a cryogen spurt to the skin surface for an appropriately short period of time (10 to 100 milliseconds), the epidermis can be precooled prior to the application of the laser pulse and, therefore, reduce or eliminate undesirable skin damage.

Despite the commercial use of cryogen spray cooling (CSC) during PWS laser therapy, there is still a limited understanding of the fluid dynamics, thermodynamics, and heat transfer characteristics of cryogen sprays. Optimization of CSC has become necessary after clinical studies have shown that current CSC commercial nozzles provide insufficient epidermal protection to patients with higher epidermal melanin concentration. To achieve this goal, it is necessary to explore the influence that fundamental spray properties have on the overall heat extraction from skin ( $Q$ ) and the instantaneous heat flux ( $q$ ).

In this work we present recent experimental studies targeted towards the characterization of cryogen sprays and the optimization of cooling procedures. To do that, we measure the average droplet diameter ( $d$ ), velocity ( $v$ ), and droplet density ( $C$ ) with the aid of a phase Doppler particle analyzer (PDPA). We also measure the overall mass flux ( $m$ ), and average spray temperature ( $T$ ). Finally, using

custom-built temperature sensor devices, we compute  $Q$  and  $q$ .

We show that  $q$  is largely dominated by  $m$  and  $v$ , and not so much by other spray characteristics, such as  $d$  and  $T$ , as previously believed. Moreover, show that less dense sprays appear to induce higher  $q$ . We go on to show that among  $m$  and  $v$ , the former has an even stronger influence on  $Q$  and  $q$  than the latter.

### INTRODUCTION

During dermatologic laser treatments of vascular lesions, such as port-wine stains (PWS), laser light absorbed by the epidermal melanin poses two obstacles. First, if a significant portion of energy from the laser is absorbed within the epidermis, it may cause irreversible thermal damage to the epidermis and, second, light absorption in the epidermis results in less energy reaching the target vessels [1]. Cryogen spray cooling (CSC) is used effectively on patients with low melanin concentration (skin types I-IV) to prevent epidermal thermal damage, while allowing sufficient energy to reach the target lesion [2,3,4]. However, CSC fails to provide sufficient thermal protection for patients with darker skin types (V and VI), who have higher levels of epidermal melanin. Therefore, to extend the benefit of CSC to all patients, it is necessary to improve cooling efficiency: this can be achieved by an in depth understanding of the fundamental spray parameters that influence heat extraction from human skin.

In recent studies, it has been shown that  $q$  can be increased by changing nozzle geometry, such as nozzle diameter [3,5,6], spray conditions, such as nozzle-to-skin distance [7], and/or sequential deposition of cryogen in multiple spurts [8]. The reason is that changes of these parameters influence the fundamental spray properties ( $m$ ,  $d$ ,  $v$ ,  $C$ , and  $T$ ). Depending on how these properties combine, the net

effect on  $q$  may be different. Therefore, to improve the efficiency of CSC and propose improved nozzle designs and spray conditions, it is important to ascertain which of the fundamental spray properties have the greatest influence on the overall heat extraction through the skin surface.

In this study we first show the spray characteristics and heat extraction as a function of nozzle-to-skin distance from a typical commercial nozzle. Then, using spray nozzles with inner diameter (I.D.) varying from 0.8 to 1.4 mm, we show the impact on  $q$  resulting from variations in the nozzle diameter. For each of the sprays produced by these nozzles we measure the overall mass flow rate ( $\dot{m}$ ), average droplet diameter ( $d$ ), velocity ( $v$ ), droplet density ( $C$ ), and temperature ( $T$ ). We then establish a correlation of each of these properties with the overall ( $Q$ ) and maximum ( $q_{max}$ ) heat extracted as the spray is directed upon a flat surface temperature sensor. We then conduct a parametric study. By doing this we are able to discern the contribution of the two most influential properties on  $q_{max}$ . Finally, we propose nozzle design improvements and spraying conditions based on these findings.

## EXPERIMENTAL PROCEDURES

### Cryogen Delivery and Nozzle Configurations

A total of four nozzles and three valves were used to provide six different valve/nozzle combinations. The four nozzles used for this study include: Two commercial cryogen spray nozzles used for laser treatment of vascular lesions and hair removal (ScleroPLUS™, and GentleLASE™, Candela, Wayland, MA), with inner diameters (I.D.) of 0.8 and 0.5 mm, respectively; and two custom made nozzles, narrow and wide, with I.D. of 0.7 and 1.4 mm, respectively. Liquid cryogen (tetrafluoroethane, boiling temperature  $T_b = -26$  °C at atmospheric pressure) was delivered through a standard high-pressure hose connected to a control valve. The container was pressurized at the cryogen saturation pressure (670 kPa at 25 °C). Solenoid valves were used to provide 100 ms spurts.

Two of the three valves tested operate on an open/close only system and, therefore, for a given spurt, each valve/nozzle configuration has only one characteristic mass flux associated with it. By using a voltage controlled analog valve (Parker Hannifin Corporation, Pneutronics Div., Hollis, NH) attached to the GentleLASE™ nozzle, we were able to vary the mass flux ( $\dot{m}$ ) from 45 to 110 g/min. These mass

fluxes correspond to the maximum and minimum valve constrictions, respectively. Table 1 provides a detailed description of each valve/nozzle configuration.

Nozzle	I.D. (mm)	Length (mm)	Solenoid Valve
ScleroPLUS™ (SP)	0.8	--	Parker-Hannifin, Grl Valve Div, S. 99
GentleLASE™ (GL)	0.5	25	Parker-Hannifin, Grl Valve Div, S. 99
Narrow (N)	0.7	25	Fuel injector
Wide (W)	1.4	25	Fuel injector
GentleLASE™ (GL)	0.5	25	Analog Valve (AV) @ 3.83 V, Parker Hannifin, Pneutronics Div
GentleLASE™ (GL)	0.5	25	Analog Valve (AV) @ 11.34 V, Parker Hannifin, Pneutronics Div

**Table 1:** Valve/nozzle configurations used in this study.

### Mass flux measurements

A 12 oz cryogen container was connected to each valve/nozzle configuration listed in Table 1. To compute the mass flux ( $\dot{m}$ ), the valve was opened and cryogen was released continuously for 1-2 min. The times for which the valve remained open and the weight loss of the containers after each spurt were recorded. Three experiments were carried out for each valve/nozzle configuration and good agreement was obtained among all measurements. Considering all sources of error, a 5% uncertainty is estimated for all the values of  $\dot{m}$  measured. Since sprays produced by these valve/nozzle configurations reach fully developed conditions within 30 ms [6], it is reasonable to assume that the  $\dot{m}$  measured for these continuous sprays are similar to those corresponding to 100 ms spurts.

### Droplet Diameter, Velocity, and Concentration

A Phase Doppler Particle Analyzer (PDPA by TSI Inc, St. Paul, MN) was used to obtain the local average droplet diameter ( $d$ ), velocity ( $v$ ), and droplet density in droplets/cm<sup>3</sup> ( $C_{droplet}$ ) of continuous cryogen sprays. The PDPA operates by producing a probe volume, typically smaller than 1 mm<sup>3</sup>, at the intersection of two off-phase laser beams of the same wavelength. As a droplet passes through the probe volume, the interference fringe pattern produced by intersecting beams is projected onto the off-axis detectors. The frequency shift of the fringe pattern is proportional to droplet velocity and the phase difference between the

signals collected by each detector is proportional to droplet diameter. The number of droplets crossing the probe volume is simultaneously recorded to measure  $C_{droplet}$ . Further details about the operation of this device may be found elsewhere [9]. All PDPA measurements were taken at a distance of 60 mm from the nozzle tip.

### Temperature Measurements

A type-K thermocouple with bead diameter of approximately 0.3 mm and response time of ~ 40 ms (SSC-TT-E-36 by Omega, Stamford, CT) was used to measure local average steady-state spray temperature. The thermocouple was held in place by a thin rigid wire to minimize spray disruption. Since water condensation and freezing on the thermocouple bead could affect temperature measurements, experiments were conducted in a chamber filled with dry air (relative humidity below 5%). Similar to the PDPA measurements, average spray temperatures were taken at a distance of 60 mm from the nozzle tip, a typical distance during CSC laser dermatologic surgery.

### Heat flux measurements

A custom-made device similar to those reported previously [7,8] was designed and built to measure the maximum heat flux ( $q_{max}$ ), and the total heat removed ( $Q_{total}$ ) by a 100 ms spurt for all valve/nozzle configurations used in this study. The device consists of a silver disk (3.18 mm diameter, 0.17 mm thickness), thermally insulated by epoxy ( $k_T=0.218$  W/m-K). The top surface of the disk was exposed to the cryogen spray and the temperature of the disk was measured by a type-K thermocouple soldered to the bottom side (Figure 1). The disk temperature was assumed to be uniform due to the high thermal conductivity of silver ( $k_T = 429$  W/m-K). With these temperature measurements,  $q_{max}$  in  $W/cm^2$  was computed by the following equation:

$$q_{max} = \frac{m_{disk} c_{disk} \left( \frac{dT_{disk}}{dt} \right)_{max}}{A_{disk}} \quad (1)$$

where  $m_{disk}$ ,  $c_{disk}$ ,  $T_{disk}$ ,  $A_{disk}$  are the mass (kg), specific heat (J/kg-K), the temperature (K), and the exposed surface area of the silver disk ( $cm^2$ ), respectively, and  $\left( \frac{dT_{disk}}{dt} \right)_{max}$  represents the maximum rate of temperature change during the spurt.

To compute  $Q_{total}$  produced by each valve/nozzle configuration in  $J/cm^2$ , we used the following equation:

$$Q_{total} = \frac{m_{disk} c_{disk} (T_0 - T_{disk(t=160ms)})}{A_{disk}}, \quad (2)$$

where  $T_0$  is the initial disk temperature and  $T_{disk(t=160ms)}$  is the disk temperature 160 ms after the start of the spurt. The latter value of  $T$  was chosen because for all the valve/nozzle configurations used in this study, 160 ms was a sufficiently long time where no further variation in the disk temperature was recorded, i.e., where  $\frac{dT_{disk}}{dt} = 0$ .

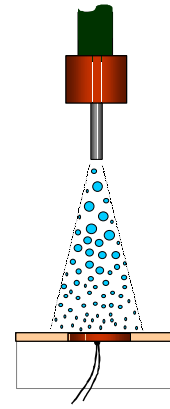


**Figure 1:** The heat flux measurement device consists of a thin silver disk, embedded in a thin epoxy plate and supported by polyurethane foam. A thermocouple measures temperature variation of the silver disk while its front surface is exposed to the cryogen spray.

## RESULTS

### Nozzle-to-skin distance

Figure 2 shows the average droplet diameter ( $d$ ), velocity ( $v$ ), temperature ( $T$ ) and heat transfer coefficient ( $h$ ) as a function of  $z$  for sprays from the GL nozzle controlled by the open/close digital valve. As seen in Figure 2a, the maximum droplet diameter for is  $d_{max} = 8 \pm 0.2$  mm, measured at  $z = 60$  mm. The measurements of  $v$  for the same nozzle are presented in Figure 2b. These results show a similar behavior to that of  $d$ , with an increasing trend within the first 30 mm from the nozzle. At larger distances,  $v$  decreases, reaching 10 m/s at  $z = 200$  mm.

Measurements of  $T$  are depicted in Figure 2c. An extrapolation of the temperature trend indicates that the exit temperature,  $T_0$ , is around  $-48$  °C. The minimum temperature,  $T_{min}$ , is around  $-58$  °C, reached at  $z = 80$  mm, and  $T$  starts to increase at  $z > 80$  mm.

Finally, Figure 2d shows the variation of  $h$  with  $z$ . The values shown represent averages over the duration of the spurt (100 ms) as well as over the detector area. After reaching a maximum value of  $h_{max} \approx 6,200$  W/m<sup>2</sup>K at  $z = 50$  mm,  $h$  decreases to about 200 W/m<sup>2</sup>K at  $z = 120$  mm. These results show that there is no obvious correlation between,  $d$ ,  $v$ , and  $T$  with  $h$ .

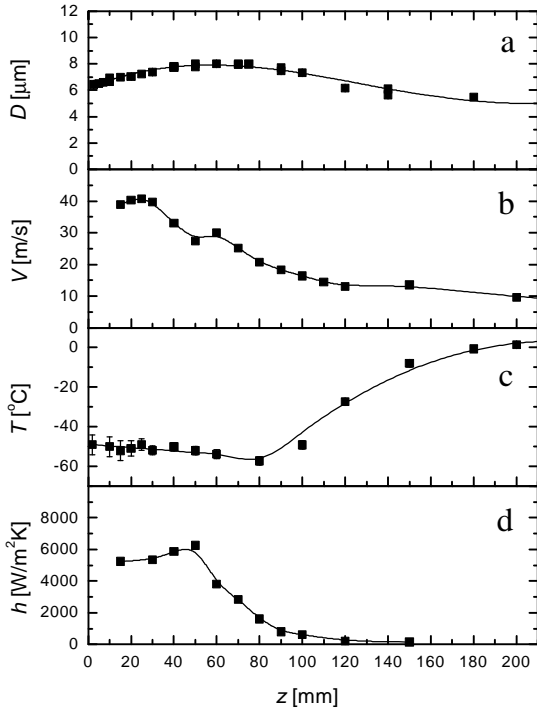


**Fig.2:** Average droplet diameter ( $d$ ), velocity ( $v$ ), temperature ( $T$ ) and heat transfer coefficient ( $h$ ), measured as a function of distance from the nozzle tip ( $z$ ) for the 0.5 mm nozzle.

### Diameter Effect

Figure 3 shows the maximum rate of temperature change,  $\left(\frac{dT_{disk}}{dt}\right)_{max}$ , for the wide (W) nozzle and the

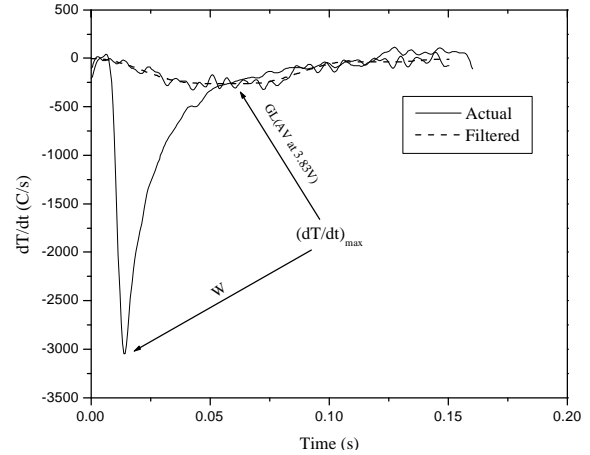
GentleLASE™ (GL) nozzle controlled by the analog valve at 3.83 V. These valve/nozzle configurations produced the largest and smallest  $\left(\frac{dT_{disk}}{dt}\right)_{max}$ ,

respectively, of all the valve/nozzle configurations.

These results show that there is a large effect of the nozzle diameter on the heat flux. This is an important finding from a practical point of view. However, it does not tell us which of the spray characteristics has the largest impact on the heat extraction.

### Heat Flux and Mass Flux

Figure 4 illustrates mass flux ( $\dot{m}$ ) and total heat removed ( $Q_{total}$ ) by each valve/nozzle configuration. The  $Q_{total}$  ranges from 0.8 to 2.4 J/cm<sup>2</sup>. The  $Q_{total}$  measurements show the total heat extracted by a 100 ms spurt if sufficient time was allowed for all the heat



extraction by a single spurt to occur.

**Figure 3:** Maximum heat flux  $(dT/dt)_{max}$  is shown for the W nozzle and the GentleLASE nozzle used with an AV at 3.83 V as a function of time beginning at the start of a 100 ms cryogen spurt.

As seen in Figure 4,  $\dot{m}$  varies by a factor of 3. A factor of 3 variation was also seen in  $Q_{total}$  amongst all the valve/nozzle configurations. Figure 5 shows the maximum heat flux ( $q_{max}$ ) and  $\dot{m}$  produced by the GentleLASE nozzle at the two different voltages applied to the AV. Using this approach, we see that  $q_{max}$  also varies proportionally with  $\dot{m}$ .  $q_{max}$ , however, varies by a factor of 11 for the valve/nozzle configurations used for this study.  $q_{max}$  is the focus of this study due to its importance in dynamic cooling during port-wine stain laser therapy.

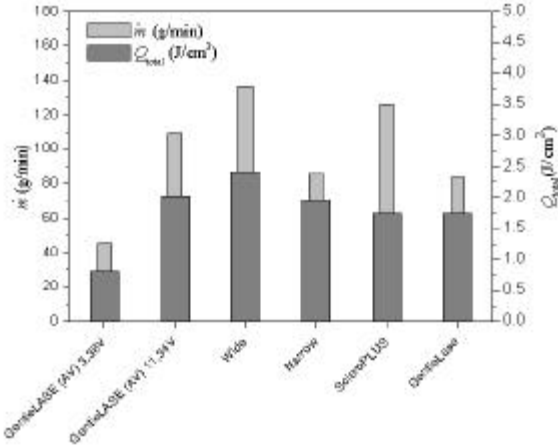


**Figure 4:** The mass flux and the total heat removed produced by each valve/nozzle configuration.

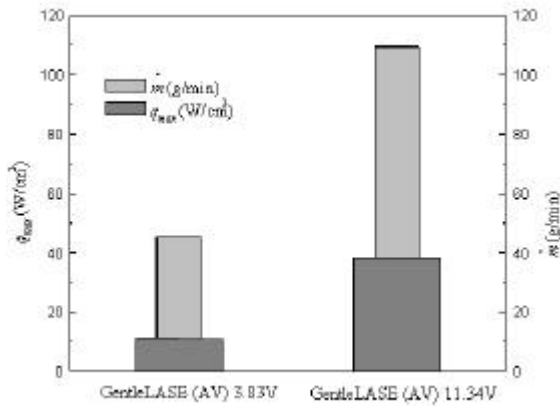


**Figure 5:** The proportional changes in  $q_{\max}$  and mass flux are shown for the GentleLASE nozzle with the analog valve (AV) at applied voltages of 3.83 V and 11.34 V.

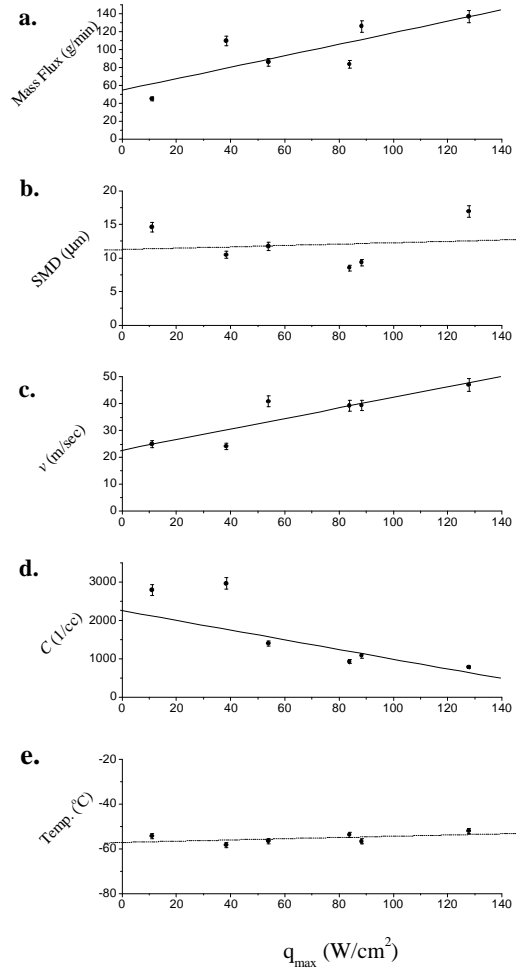


**Figure 6:** (a) Mass flux, (b) Sauter Mean Diameter (SMD), (c) Average droplet velocity ( $v$ ), (d) Droplet concentration ( $C_{\text{droplet}}$ ), and (e) Average spray temperature are shown as a function of the maximum heat flux ( $q_{\max}$ ). The order of the valve/nozzle configurations labeled in (a) remains the same for all graphs (b-e).

Figure 6a\* illustrates  $\dot{m}$  as a function of  $q_{\max}$ . This figure displays a trend of increasing  $q_{\max}$  with an increase in  $\dot{m}$ . The lowest value of  $\dot{m}$  (45 g/min) was delivered by the GentleLASE nozzle with the AV at 3.8 V, and this configuration also produced the smallest value of  $q_{\max}$  (11.0 W/cm<sup>2</sup>). The W nozzle delivered the highest  $\dot{m}$  (137 g/min) and also produced the highest  $q_{\max}$  (128 W/cm<sup>2</sup>).

### Droplet Diameter, Velocity, and Concentration

Figure 6b\* shows Sauter Mean Diameter (SMD) as a function of the  $q_{\max}$ . No correlation is apparent between the SMD and  $q_{\max}$ , the variations in the SMD range from 9 to 17  $\mu\text{m}$ . Although not apparent, for

\* For convenience Figures 5 & 6 present the maximum heat flux ( $q_{\max}$ ), which is the dependent parameter, on the shared horizontal axis.

each valve/nozzle configuration and for a fixed distance from the nozzle, there is a large variation in droplet size distribution of as much as 35-40% from the average diameter, with single droplet measurements ranging from less than 1  $\mu\text{m}$  to greater than 50  $\mu\text{m}$ .

Figure 6c\* shows average droplet velocity ( $v$ ) as a function of  $q_{\text{max}}$ . An increase in  $v$  results in an increase in  $q_{\text{max}}$ . The range of  $v$  measured varies from 24 to 47 m/s. Figure 6d\* illustrates  $q_{\text{max}}$  as a function of the droplet concentration ( $C_{\text{droplet}}$ ). This figure presents an inversely proportional relationship between  $q_{\text{max}}$  and  $C_{\text{droplet}}$ , with the latter ranging from 780 to 3000  $1/\text{cm}^3$ .

### Temperatures

Figure 6e\* shows small variations in temperature relative to the large changes in the heat flux. The temperatures ranged from  $-52$  to  $-58$   $^{\circ}\text{C}$  showing minimal variation relative to other parameters in this study.

## DISCUSSION

### Nozzle Design

The droplet diameter growth seen in Figure 3a between  $0 < z < 60$  mm, is an indication of droplet coalescence [10,11], a phenomenon which may contribute more to the average droplet diameter variation than the evaporation process. However, evaporation becomes the dominant process in determining the average droplet size for  $z > 60$  mm, as demonstrated by decreasing  $D$  at larger  $z$ .

The increase of  $V$  within the first 30 mm (Figure 3b), can be explained by the coalescence of large fast droplets, with slower smaller ones. The decrease of  $V$  for  $z > 30$  mm results from droplet deceleration due to drag as droplets move through quiescent air [12,6]. Clearly, the complexity of the problem is such that establishing a correlation between  $D$ ,  $V$ ,  $T$ , and  $h$ , is not straightforward, following this approach. This study shows that large variations of  $h$  can be achieved by positioning the nozzles at different distances.

### Nozzle Diameter Effect

Apparently, nozzle I.D. has a large impact on  $q$ . However, one should be aware that if no provision were taken, changing I.D. would also affect  $m$  and the other spray properties.

We observed a three-fold variation in the total heat removed ( $Q_{\text{total}}$ ) and a proportional three-fold variation in mass flux ( $\dot{m}$ ) (Figure 3). The only exception in Figure 4 corresponds to the ScleroPLUS valve/nozzle configuration. We believe this may be due to repairs needed for the valve between experiments with this nozzle, resulting in some inconsistent performance.

As shown in Figure 6a, there is a strong dependence of  $q_{\text{max}}$  on  $\dot{m}$ . This proportional relationship was also observed in measurements of surface cooling using a water spray [13]. Varying  $\dot{m}$  by a factor of three results in a similar variation in  $Q_{\text{total}}$  (Figure 4) and shows an even larger variation in  $q_{\text{max}}$  (factor of 11) (Figure 5). A similar range of values for heat flux was obtained in an earlier study using the insulated copper rod method for narrow and wide nozzles [14].

For more efficient CSC during laser therapy of PWS, however, the rate of heat removal is crucial. Increasing the rate of heat removal improves spatial selectivity (keeping the epidermis cool, while raising the temperature of the target blood vessels). Faster cooling prevents the temperature reduction caused by CSC to reach the targeted blood vessels. For this reason, the maximum heat flux ( $q_{\text{max}}$ ) measured in  $\text{W}/\text{cm}^2$  was studied in more detail in this paper.

$q_{\text{max}}$  showed no dependence on the SMD (Figure 6b) in the measurements obtained in this study. This may be due to a wide distribution of droplet diameters measured, with diameters varying up to 40% with respect to the average droplet diameter. Large variations in the SMD with modest variation in heat flux were also reported in [15]. More data points and larger variations in the heat flux are necessary to observe any dependencies that may exist.

Larger values of  $v$  correlate to greater values for  $q_{\text{max}}$  (Figure 6c). Similar trends were observed in an earlier study [16] in which the heat flux increased with an increase in droplet velocity. This relationship between droplet velocity and heat transfer coefficient (i.e. heat flux) was also observed in a study on surface cooling with a water spray [13]. This may be due to the ability of faster droplets of the same size to penetrate deeper into the liquid cryogen layer that forms on the skin surface during CSC [5]. It may also be attributable to the effect of the axial velocity transferring to a radial velocity of the liquid cryogen moving over the surface, thus enhancing the convective heat transfer coefficient. Within the

confines of the valve/nozzle configurations used in this study, increasing  $\dot{m}$  produced higher  $v$ . The co-dependence of heat extraction on the two related parameters,  $\dot{m}$  and  $v$ , is being explored in our current work.

Figure 6e shows modest changes in spray temperature, measured at a distance of 60 mm from the nozzle tip for all valve/nozzle configurations. Due to the small variations in the spray temperature seen in the confines of this study, it is clear that the spray temperature does not heavily influence the heat flux values measured.

Figure 7 shows the percent change in the average velocity relative to the percent change in the heat flux. Each set of bars corresponds to two different valve/nozzle diameter configurations for which the mass output differences were minimal (< 4%), as depicted on the x-axis. As seen, even though the average droplet velocity may vary as much as 100% between two configurations, there is only a modest variation of less than 20% in heat flux. These results suggest that the effect of  $v$  on  $Q$  and  $q_{max}$  should be modest compared to the effect of  $m$ .

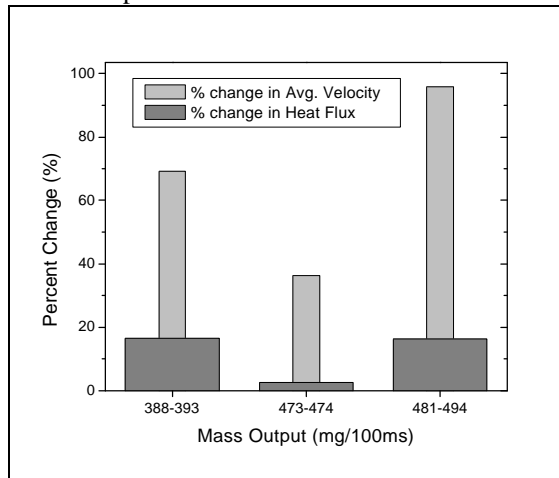


**Figure 7:** Preliminary data showing the relatively large changes in the average droplet velocity resulting in modest changes in the heat flux.

## CONCLUSIONS

In this study, it is shown that the heat extracted from a surface using CSC is proportionally influenced by the cryogen mass flux. A three-fold variation was measured for the total heat removed by a 100 ms spurt amongst all the valve/nozzle configurations, corresponding to a proportional three-fold variation in the mass flux. Even larger variations were observed in the maximum heat flux (factor of 11). Keeping the nozzle geometry constant, it is shown that increasing the mass flux can proportionally increase the heat

flux. It appears that the spray parameters that have the largest effect on the heat extraction rate are the mass flux and average droplet velocity, which show a proportional relationship, while an inversely proportional relationship exists between the droplet concentration and the heat flux. No correlation between heat flux and droplet size could be deduced from the measurements obtained in this study. Based on these results, it appears that in order to improve the heat extraction rate of current nozzle designs, one should focus on maximizing the spurt mass flux more than the average droplet velocity, which could be achieved simply by increasing the nozzle diameter. The end result of this will be the improvement of CSC, enabling the port wine stain laser therapy for patients with higher melanin concentration.

## REFERENCES

- 1 Chang CJ, Nelson JS. Cryogen spray cooling and higher fluence pulsed dye laser treatment improve port-wine stain clearance while minimizing epidermal damage. *Dermatol. Surg.* 1999; 25: 767-772.
- 2 Nelson JS, Milner TE, Anvari B, Tanenbaum BS, Kimel S, Svaasand LO, Jacques SL. Dynamic epidermal cooling during pulsed laser treatment of port-wine stain. A new methodology with preliminary clinical evaluation. *Arch. Dermatol.* 1995; 131: 695-700.
- 3 Anvari B, Tanenbaum BS, Milner TE, Kimel S, Svaasand LO, Nelson JS. A theoretical study of the thermal response of skin to cryogen spray cooling and pulsed laser irradiation-implications for treatment of port-wine stain birthmarks. *Phys. Med. Biol.* 1995; 40: 1451-1465.
- 4 Welch AJ, Motamedi M, Gonzalez A. Evaluation of cooling techniques for the protection of the epidermis during Nd:YAG laser irradiation of the skin. *Nd-YAG Lasers in Surg. and Med.* 1983; New York: Elsevier.
- 5 Verkruysse W, Majaron B, Aguilar G, Svaasand LO, Nelson JS. Dynamics of cryogen deposition relative to heat extraction rate during cryogen spray cooling. *Proceedings SPIE* 2000; 3907: 37-58.
- 6 Aguilar G, Majaron B, Verkruysse W, Nelson JS, Lavernia EJ. Characterization of cryogenic spray nozzles with application to skin cooling. *Proceedings of the ASME* 2000; Fluids Engineering Division: 189-197.
- 7 Aguilar G, Majaron B, Pope K, Svaasand LO, Lavernia EJ, Nelson JS. Influence of nozzle-to-skin distance in cryogen spray cooling for

- 
- dermatologic laser surgery. *Lasers in Surg. and Med.* 2001; 28: 113-120.
- 8 Majaron B, Aguilar G, Basinger B, Randeberg LL, Svaasand LO, Lavernia EJ, Nelson JS. Sequential cryogen spraying for heat flux control at the skin surface. *Proceedings SPIE* 2001; 4244: 74-81.
  - 9 Bachalo WD, Houser MJ. Analysis and testing of a new method for drop size measurement using laser light scatter interferometry. Prepared for National Aeronautics and Space Administration, Lewis Research Center under contract NAS3-23684.
  - 10 Orme M, Experiments on droplet collisions, bounce, coalescence and disruption. *Progress in Energy and Combustion Science* 1997; 23:65-79.
  - 11 Nishitani R, Kasuya A, and Nishina Y. In situ STM observation of coalescence of metal particles in liquid, *Zeitschrift fur Physik D* 1993; 26:S42-S44.
  - 12 Aguilar G, Majaron B, Verkruysse W, Zhou Y, Nelson JS, Lavernia EJ. Theoretical and experimental determination of droplet diameter, temperature, and evaporation rate evolution in cryogenic sprays. *Int J Heat Mass Tran* 2000; 44:3201-3211.
  - 13 Schmidt J, Boye H. Influence of velocity and size of the droplets on the heat transfer in spray cooling. *Chem. Eng. Technol.* 2001; 24: 255-260
  - 14 Aguilar G, Verkruysse W, Majaron B, Svaasand LO, Lavernia EJ, and Nelson JS. Measurement of heat flux and heat transfer coefficient during continuous cryogen spray cooling for laser dermatologic surgery. *IEEE J Sel Top Quantum* 2001; 7:1013-1021.
  - 15 Pikkula BM, Torres JH, Tunnell JW, and Anvari B. Cryogen spray cooling: effects of droplet size and spray density on heat removal. *Lasers in Surgery and Medicine* 2001; 28: 103-112.
  - 16 Anvari B, Pikkula BM, Tunnell JW, Torres JH. Thermal and fluid characteristics during cryogen spray cooling. *Proceedings SPIE* 2001; 4244: 105-112.